



HAL
open science

Mechanofluorochromism of a Difluoroboron- β -Diketonate Derivative at the Nanoscale

Marine Louis, Cristian Pinëro García, Arnaud Brosseau, Clémence Allain, Rémi Métivier

► To cite this version:

Marine Louis, Cristian Pinëro García, Arnaud Brosseau, Clémence Allain, Rémi Métivier. Mechanofluorochromism of a Difluoroboron- β -Diketonate Derivative at the Nanoscale. *Journal of Physical Chemistry Letters*, 2019, 10 (16), pp.4758-4762. <10.1021/acs.jpcllett.9b01923>. <hal-02319855>

HAL Id: hal-02319855

<https://hal.science/hal-02319855v1>

Submitted on 21 Oct 2019

HAL is a multi-disciplinary open access archive for the deposit and dissemination of scientific research documents, whether they are published or not. The documents may come from teaching and research institutions in France or abroad, or from public or private research centers.

L'archive ouverte pluridisciplinaire **HAL**, est destinée au dépôt et à la diffusion de documents scientifiques de niveau recherche, publiés ou non, émanant des établissements d'enseignement et de recherche français ou étrangers, des laboratoires publics ou privés.



HAL Authorization

Mechanofluorochromism of a Difluoroboron- β -Diketonate Derivative at the Nanoscale

Marine Louis, Cristian Piñero García, Arnaud Brosseau, Clémence Allain,* and Rémi Métivier*

PPSM, ENS Paris-Saclay, CNRS, Université Paris-Saclay, 94235 Cachan, France

ABSTRACT: Mechanofluorochromic nanoparticles have been prepared from a difluoroboron β -diketonate complex, and their behavior has been investigated at the nanoscale using atomic force microscopy (AFM) coupled with fluorescence spectroscopy. Two types of nanoparticles were observed, associated with green and yellow emission, reflecting the crystalline polymorphism of this material. While the green-emitting nanoparticles are mechanically insensitive under our conditions, the yellow-emitting ones display a marked hypsochromic shift upon shearing with the AFM tip. At the macroscopic level, the grinding of the bulk material is attributed to the amorphization of the crystalline powder. On the contrary, the marked mechanofluorochromism observed at the nanoscale is attributed to a crystal-to-crystal phase transition. This specific behavior at the nanolevel is extremely promising for applications such as nanoproboscopes of local mechanical stress.

Mechanofluorochromism refers to compounds or materials for which the fluorescence spectra can be modified under mechanical stress (shearing, grinding, smearing, stretching, etc.). Since the first publications in the 2000s,¹⁻³ the field has attracted considerable interest, and various systems have been described: ⁴ organic compounds,⁵ organometallic complexes,⁶ and polymers.⁷ However, most of the studies focus on only bulk powders and materials, and very few studies have been reported on the design and investigation of nanoparticles.⁸⁻¹⁰ This topic is of major interest for the development of smart fluorescent (nano)materials with the possibility of revealing specific effects of the mechanofluorochromic behavior due to the increase of the surface-to-volume ratio, such as spatial amplification (the so-called “domino-like effect”)¹¹ or enhancement by photophysical processes (namely, “giant amplification” by multiple energy transfer pathways).¹² It also offers appealing perspectives in mechanobiology with the possibility to create new tools to probe biological forces at the cell level.^{13,14} Two first examples, reported in 2013 by Kobayashi et al.⁸ and in 2017 by Fischer et al.,⁹ describe spectral shifts of the emission spectra of conjugated polymer nanoparticles and quantum dots, respectively, upon application of a compression force induced by an AFM tip. A third example reported by Sagara et al.¹⁰ describes the synthesis and preparation of mechanoresponsive micelles covalently linked to glass beads that are stimulated at the macroscale by vortexing the suspension. However, to the best of our knowledge, the comparison, for a given compound, of the mechanofluorochromism at the macroscale (by grinding a crystalline powder) and at the nanoscale (by applying shearing stress using an AFM tip on nanoparticles) has never been studied, while it appears of utmost importance to understand the phenomenon and its specific size-dependent effects. Among the different families of molecules identified for their bright fluorescence properties, the difluoroboron β -diketonate derivatives are well-known for their mechanofluorochromic behavior.¹⁵⁻¹⁷ Several studies have investigated their properties at the nanoscale for application in biological imaging^{18,19} and as oxygen sensors,²⁰⁻²⁴ but no report has been published related to the potential mechanofluorochromic behavior of these nanoparticles.

Our research focuses on the study of a difluoroboron β -diketonate derivative to explore the influence of mechanical stress on the emission properties at the nanoscale. We describe here the preparation and characterization of nanoparticles. A complete study, down to the single-nanoparticle level, performed via a setup coupling AFM and fluorescence spectroscopy, allows us to highlight for the first time the specific fluorescence response induced by mechanical stress at the nanoscale on this family of materials.

The **DFB-Bu-Amide** derivative is introduced in Figure 1a. In a previous paper,²⁵ the mechanofluorochromic behavior of this compound in the bulk state was fully detailed and its polymorphic nature was described. Two crystalline polymorphs were identified: a green-emissive one ($\lambda_{\text{maxem}} \approx 480$ nm) and a yellow-emissive one ($\lambda_{\text{maxem}} \approx 510$ nm), both present in different proportions in the crystalline powders isolated after purification. A yellow/orange-emissive amorphous phase ($\lambda_{\text{maxem}} \approx 540$ nm), generated by grinding the powder in a mortar, was also outlined, as evidenced by powder X-ray diffraction before and after grinding (cf. Figure 1c).

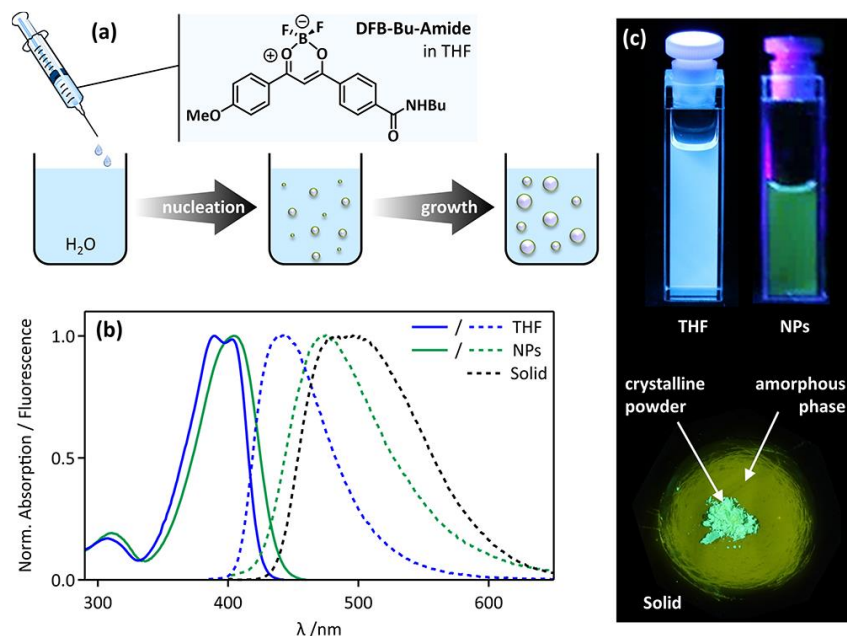


Figure 1. (a) **DFB-Bu-Amide** structure and description of the reprecipitation method used for preparation of the nanoparticles. (b) Absorption spectra (full lines) and emission spectra (dotted lines) of **DFB-Bu-Amide** in THF solution (blue lines), as a suspension of nanoparticles in H₂O/THF 80:20 (green lines), and in the solid state (black line). (c) Photographs of the fluorescence of **DFB-Bu-Amide** in THF solution, as a suspension of nanoparticles, and in the solid state (green-emissive crystalline powder in the center and yellow/orange-emissive amorphous phase obtained after grinding).

The nanoparticles were prepared by the reprecipitation method in a H₂O/THF 80:20 mixture (Figure 1a). This method offers a quick and simple way to yield pure organic nanocrystals. The absorption spectrum of the nanoparticles is relatively similar to the one obtained in THF solution (Figure 1b), however, with a disappearance of the vibrational structure and a slight red shift of the absorption maxima (~ 950 cm⁻¹), indicating weak interactions between the molecules, in the ground state, within the nanoparticles. On the contrary, the emission spectra are significantly different (Figure 1b). The Stokes shift is increased, from 3000 cm⁻¹ for the THF solution to 3650 cm⁻¹ for the nanoparticles. Interestingly, the nanoparticles' emission spectrum is located halfway between the ones in THF solution and in the crystalline powder; this preparation method seems to favor the formation of the green emitting crystalline polymorph. A dramatic decrease of the fluorescence quantum yield is however observed (0.06 in nanoparticles, compared to 0.86 in THF solution and 0.38 in crystalline solid, as shown in Table 1), which can be explained by the surrounding water medium in the colloidal state.

In order to investigate the mechanofluorochromic behavior of the nanoparticles, they were first deposited on cover-glass substrates and then studied by means of a setup coupling AFM and fluorescence microscopy equipped with an EMCCD camera and a CCD spectrograph (Figure 2a). The response of the nanoparticles under mechanical stress, which was applied via the tip of the AFM, can be investigated, as described later.

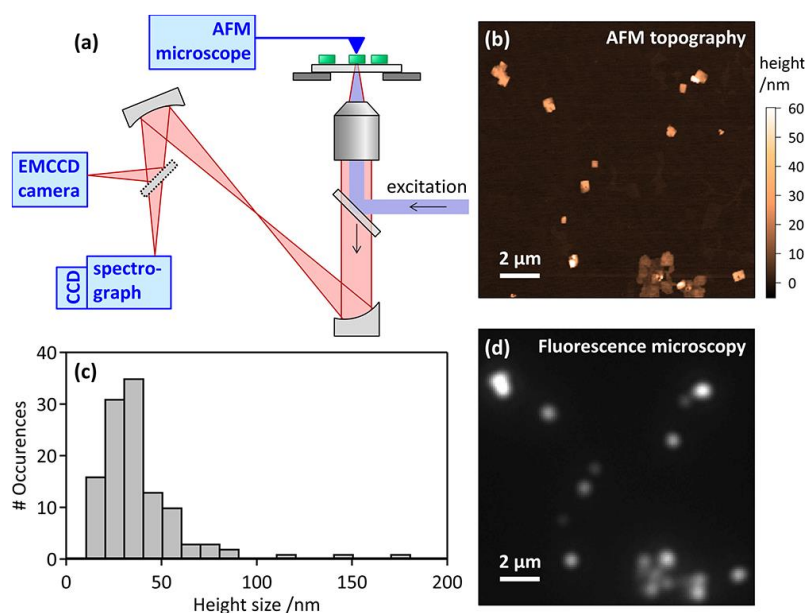


Figure 2. (a) Scheme of the experimental setup coupling AFM and fluorescence microscopy. (b) AFM topography image, (c) histogram of height sizes, and (d) correlated fluorescence microscopy image of **DFB-Bu-Amide** nanoparticles deposited on a glass coverslide.

The setup was initially used to image the nanoparticles. As displayed in Figure 2b, a significant dispersity of sizes and shapes of nanoparticles are observed, which is often the case for nanoparticles produced by the reprecipitation method. Most of the nanoparticles have a platelet-like shape, with a height size, along the z axis, between 10 and 80 nm (Figure 2b,c). A small number of particles or aggregates with height sizes larger than 100 nm can be found in some areas.

Well-separated single nanoparticles could be further investigated by fluorescence spectroscopy on a single-particle basis. The wide-field fluorescence image of the nanoparticles was accurately correlated to the AFM image (Figure 2b,d), such that each fluorescence spot could be attributed to a well-defined nanoparticle with given sizes and shape. Then, individual fluorescence spectra of every single nanoparticle were recorded systematically. Over the 75 single nanoparticles examined by this procedure, two populations were spectroscopically identified in our samples. A large population of nanoparticles show emission maxima in the range of 500–575 nm, corresponding to yellow emission, whereas a small number of nanoparticles, with emission spectra located in the 425–500 nm intervals, represent a minor population of green-emitting nano-objects (Figure 3c). These two distinct emission modes of the nanoparticles may actually correspond to the two different crystalline polymorphs existing in the bulk powder.²⁵ The platelet-like shape of the nanoparticles supports the hypothesis of crystalline nanomaterials.

The same microscopy setup was then further employed to investigate the mechanofluorochromic behavior of the individual nanoparticles. A typical experiment is performed in three steps. First, a given nanocrystal is identified and characterized by its AFM topographic image, fluorescence image, and emission spectrum. Second, the AFM is set in contact mode with a constant vertical force of the tip (130 or 260 nN, with a $\pm 30\%$ accuracy) to trigger the mechanical stimulus on the nanoparticle. An AFM image is recorded in contact mode with a tip velocity ranging from 0.5 to 1.1 $\mu\text{m s}^{-1}$, applying a local shearing force at the surface of the nanoparticle over an area of ~ 0.2 – $0.3 \mu\text{m}^2$. Third, after the mechanical stress, the resulting shape of the nanoparticle is imaged by the AFM in tapping mode, and its fluorescence spectrum is recorded. To prevent any influence of the AFM tip on the recorded emission spectra,²⁶ the latter is displaced away from the probed area. This procedure is then repeated several times: the nanoparticle is stimulated with “AFM-based nanoshearing mechanical stress” of

increasing intensity and followed by fluorescence spectroscopy until no more evolution of the emission spectra is observed.

Table 1. Absorption and Emission Maxima and Fluorescence Quantum Yield of DFB-Bu-Amide in THF Solution, in Nanoparticles, and in the Solid State (Crystalline Powder)

	λ_{\max} (abs)	λ_{\max} (em)	ΦF
solution (THF)	390 nm	442 nm	0.86
nanoparticles (suspension in H ₂ O/THF 80:20)	405 nm	475 nm	0.06
solid state (crystalline bulk powder)		510 nm	0.38

We first investigated the emission properties of green emissive nanoparticles under mechanical stress. Unfortunately, no noticeable change in the emission spectra could be detected even after several mechanical shearing stress sequences with a 130–520 nN vertical force of the AFM tip (see the Supporting Information, Figure S1). Yellow-emissive nanoparticles proved to be much more interesting. Two representative examples, NP1 and NP2, are displayed in Figure 3a,b.

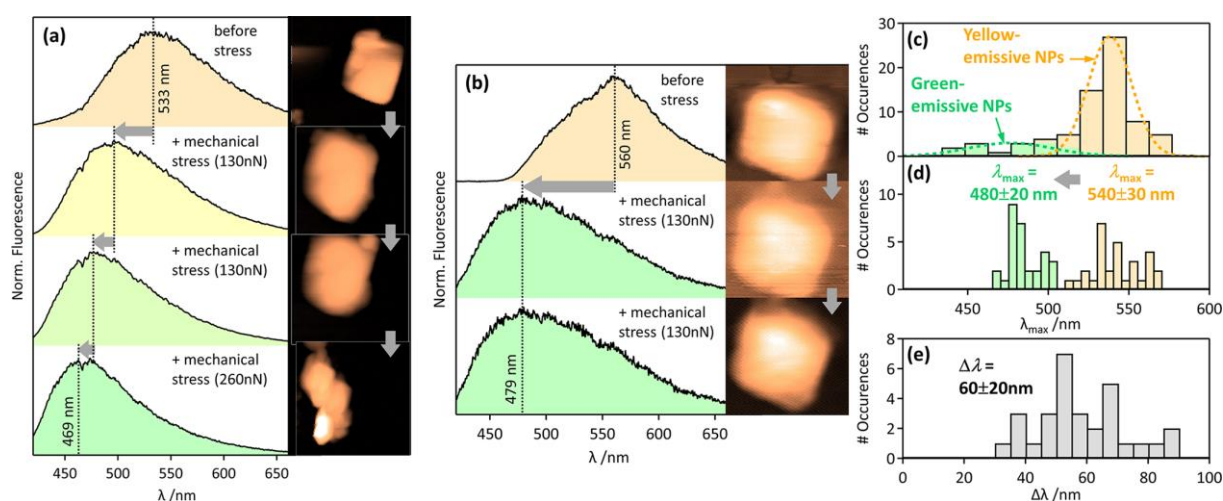


Figure 3. (a,b) Emission spectra and corresponding AFM images of two single yellow-emissive nanoparticles (a: NP1, b: NP2) before mechanical stimulation and after application of several shearing mechanical stress sequences (130 and 260 nN). Shearing stress applied by means of the AFM tip in the contact mode: tip velocity = 0.6–0.8 $\mu\text{m s}^{-1}$ on an area of $\sim 0.2 \mu\text{m}^2$. Scale-bar = 200 nm. (c) Histogram of emission maxima (λ_{\max}) of 75 isolated DFB-Bu-Amide nanoparticles. (d) Histograms of emission maxima of single nanoparticles before (yellow) and after (green) mechanical stress, obtained for 30 yellow-emissive DFB-Bu-Amide nanoparticles. (e) Histogram of the corresponding hypsochromic shift values.

The analysis of the AFM images reveals that both selected nanoparticles are platelet-shaped with an approximative global surface area of $0.16 \mu\text{m}^2$, which was well-preserved during the experiment. The initial emission spectra of NP1 and NP2 are rather different with emission maxima peaking at 533 and 560 nm, respectively. In both cases, a significant hypsochromic shift of the emission spectra (64 and 81 nm, respectively) was induced upon shearing stress applied by the AFM tip. After a complete series of mechanical stimulations, NP1 and NP2 showed similar fluorescence spectra with maxima at 469 and 479 nm, respectively (Figure 3a,b). Interestingly, these final spectra are similar to the ones measured for green-emissive nanoparticles. The rate of fluorescence change under mechanical constraint is strongly nanoparticle-dependent: in the case of NP1, the emission evolves progressively, with a gradual hypsochromic shift under increasing mechanical stimulation, whereas in the case of NP2, the blue shift of the emission is sudden and complete after only one shearing step with a vertical force of 130 nN. It is known that the shearing of a crystal is more efficient along specific planes and directions called sliding lines.²⁷ Depending on the relative orientation of the crystalline lattice axes of the nanoparticle and the mechanical stress direction, the constraints projected along

the sliding lines do not necessarily reach the level of the threshold value (namely, critical split). As a consequence, the morphology changes and the related fluorescence shifts are expected to be different from nanoparticle to nanoparticle; the full transition may be very efficient at low stimulation levels (e.g., NP2) or require much higher mechanical stress (e.g., NP1). This typical experiment was repeated for a total of 30 yellow-emissive nanoparticles, and the same mechanofluorochromic behavior was successfully demonstrated.

As an average, the investigated yellow-emissive nanoparticles displayed a maximum of emission at around 510–570 nm before any mechanical stimulation (Figure 3d). A hypsochromic shift was systematically induced under AFM-based shearing stress, from 30 up to 90 nm (average: 60 nm, as displayed in Figure 3e). Unfortunately, it has not been possible to establish any clear correlation between the size, shape, or initial fluorescence maxima and the extent of the blue shift observed after local shearing stress. It is worth noting that sometimes the integrity of the nanoparticles is not preserved; the morphology may be strongly affected after the first scans of the AFM in contact mode (see the Supporting Information, Figure S3).

Interestingly, the large mechano-induced hypsochromic effect observed at the nanoscale is in contradiction with the red shift highlighted at the macroscale (see Figure 1c). Indeed, grinding the crystalline green-emissive bulk powder always leads to a bathochromic change of the emission (~ 70 nm, 2400 cm^{-1}), and shearing the yellow-emissive crystalline phase yields the same yellow–orange emissive amorphous phase.²⁵ Therefore, our observations of nanoscale mechanofluorochromism were unexpected. Such data suggest that all of the investigated yellow-emissive nanoparticles were initially in a metastable crystalline state (Figure 3a,b). The mechanical stress applied by the AFM tip may induce a crystal-to-crystal phase transition toward the green-emissive crystalline polymorph; the mechanical stimulus of the AFM tip can favor the transformation from one crystalline form to the other, with a possible transient amorphous phase.^{11,28} Enhancement of the fluorescence intensity was frequently observed along the experiment (see the Supporting Information, Figure S2), which could be attributed to a higher fluorescence quantum yield of the green-emissive phase compared to the yellow emissive one.

The vertical force levels required to induce the emission change are larger than the ones employed in the article from Kobayashi et al., which were between 5 and 200 nN (in compression only, no shearing stress in their case).⁸ On the other side, a report from De Cola et al.²⁹ describes the use of an AFM tip to write a pattern at the surface of a millimetric crystal using its mechanofluorochromic properties, with vertical forces of around 24 μN and scan rates up to 100 $\mu\text{m s}^{-1}$. Therefore, downscaling from the macroscopic to the nanometric levels goes along with a decrease of the forces necessary to induce the mechanofluorochromic response.

In summary, we report here the preparation and study of nanoparticles of an amide-substituted difluoroboron β -diketonate derivative. After deposition of the nanoparticles on cover-glass substrates, two types of nanoparticles were investigated under the microscope and identified: green-emissive and yellow-emissive ones. Whereas the mechanical stress applied on green-emissive nanoparticles by means of a setup coupling AFM and fluorescence spectroscopy did not lead to any change of their fluorescence spectra, the analysis of yellow-emissive nanoparticles allows us to highlight for the first time a large mechanofluorochromic response at the nanoscale with this family of compounds. The AFM was used in contact mode with a constant vertical force between 130 and 260 nN to apply a shearing stress on the nanoparticles. Upon mechanical stimulation, the emission of the nanoparticles shifted from yellow to green, which could be attributed to a crystal-to-crystal phase transition. The hypsochromic shift (up to 90 nm) highlighted for the nanoparticles is at the opposite of the mechanofluorochromic properties observed at the macroscale because different processes are

involved. In the bulk powder, the crystalline-to-amorphous transition is the dominant process upon force application. Further experiments are currently in progress, such as microscopy under polarized light or simultaneous fluorescence monitoring and AFM mechanical stimulation, in order to get deeper insights into the mechanism at the origin of mechano-induced fluorescence changes and investigate this “nanomechanofluorochromism” on other derivatives. These efforts would be required to develop effective force sensors at the nanoscale as potential tools to study mechanotransduction in cellular biology, for instance.

The Supporting Information is available free of charge on the ACS Publications website at DOI: 10.1021/acs.jpcclett.9b01923. Experimental details, preparation methods, and spectroscopic and AFM data (PDF)

AUTHOR INFORMATION

Corresponding Authors

E-mail: remi.metivier@ens-paris-saclay.fr (R.M.), clemence.allain@ens-paris-saclay.fr (C.A.).

ORCID Clémence Allain: 0000-0002-2908-264X, Rémi Métivier: 0000-0001-5612-8327

Notes: The authors declare no competing financial interest.

ACKNOWLEDGMENTS

The authors acknowledge Dr. L. Bodelot from the Laboratory of Solids Mechanics at Ecole Polytechnique, France and Pr. F. Ito from the department of chemical education at Shinshuu University, Japan for fruitful discussions. The authors also acknowledge financial support of this work by the European Research Council (ERC StG MECHANO-FLUO No 715757), by the CNRS (Mission pour l'Interdisciplinarité), by the IDEX Paris-Saclay (Ph.D. fellowship to M.L.), and by the Labex CHARMMMAT (Master fellowship to C.P.G.).

REFERENCES

- (1) Löwe, C.; Weder, C. Oligo(p-phenylene-vinylene) Excimers as Molecular Probes: Deformation-Induced Color Changes in Photoluminescent Polymer Blends. *Adv. Mater.* **2002**, *14*, 1625–1629.
- (2) Ito, H.; Saito, T.; Oshima, N.; Kitamura, N.; Ishizaka, S.; Hinatsu, Y.; Wakeshima, M.; Kato, M.; Tsuge, K.; Sawamura, M. Reversible Mechanochromic Luminescence of [(C₆F₅Au)₂(m-1,4-Diisocyanobenzene)]. *J. Am. Chem. Soc.* **2008**, *130*, 10044–10045.
- (3) Sagara, Y.; Mutai, T.; Yoshikawa, I.; Araki, K. Material Design for Piezochromic Luminescence: Hydrogen-Bond-Directed Assemblies of a Pyrene Derivative. *J. Am. Chem. Soc.* **2007**, *129*, 1520–1521.
- (4) Xu, J.; Chi, Z. *Mechanochromic Fluorescent Materials: Phenomena, Materials and Applications*; The Royal Society of Chemistry, 2014.
- (5) Chi, Z.; Zhang, X.; Xu, B.; Zhou, X.; Ma, C.; Zhang, Y.; Liu, S.; Xu, J. Recent Advances in Organic Mechanofluorochromic Materials. *Chem. Soc. Rev.* **2012**, *41*, 3878–2896.
- (6) Sagara, Y.; Yamane, S.; Mitani, M.; Weder, C.; Kato, T. Mechanoresponsive Luminescent Molecular Assemblies: An Emerging Class of Materials. *Adv. Mater.* **2016**, *28*, 1073–1095.
- (7) Calvino, C.; Neumann, L.; Weder, C.; Schrettl, S. Approaches to Polymeric Mechanochromic Materials. *J. Polym. Sci., Part A: Polym. Chem.* **2017**, *55*, 640–652.
- (8) Kobayashi, H.; Hirata, S.; Vacha, M. Mechanical Manipulation of Photophysical Properties of Single Conjugated Polymer Nanoparticles. *J. Phys. Chem. Lett.* **2013**, *4*, 2591–2596.
- (9) Fischer, T.; Stottinger, S.; Hinze, G.; Bottin, A.; Hu, N.; Basche, T. Single Semiconductor Nanocrystals under Compressive Stress: Reversible Tuning of the Emission Energy. *Nano Lett.* **2017**, *17*, 1559–1563.
- (10) Sagara, Y.; Komatsu, T.; Ueno, T.; Hanaoka, K.; Kato, T.; Nagano, T. Covalent Attachment of Mechanoresponsive Luminescent Micelles to Glasses and Polymers in Aqueous Conditions. *J. Am. Chem. Soc.* **2014**, *136*, 4273–4280.
- (11) Ito, H.; Muromoto, M.; Kurenuma, S.; Ishizaka, S.; Kitamura, N.; Sato, H.; Seki, T. Mechanical Stimulation and Solid Seeding Trigger Single-Crystal-to-Single-Crystal Molecular Domino Transformations. *Nat. Commun.* **2013**, *4*, 2009.
- (12) Su, J.; Fukaminato, T.; Placial, J. P.; Onodera, T.; Suzuki, R.; Oikawa, H.; Brosseau, A.; Brisset, F.; Pansu, R.; Nakatani, K.; Metivier, R. Giant Amplification of Photoswitching by a Few Photons in Fluorescent Photochromic

Organic Nanoparticles. *Angew. Chem., Int. Ed.* **2016**, *55*, 3662–3666.

- (13) Liu, Y. L.; Qin, Y.; Jin, Z. H.; Hu, X. B.; Chen, M. M.; Liu, R.; Amatore, C.; Huang, W. H. A Stretchable Electrochemical Sensor for Inducing and Monitoring Cell Mechanotransduction in Real Time. *Angew. Chem., Int. Ed.* **2017**, *56*, 9454–9458.
- (14) Liu, Y.; Galior, K.; Ma, V. P.; Salaita, K. Molecular Tension Probes for Imaging Forces at the Cell Surface. *Acc. Chem. Res.* **2017**, *50*, 2915–2924.
- (15) Zhang, G.; Lu, J.; Sabat, M.; Fraser, C. L. Polymorphism and Reversible Mechanochromic Luminescence for Solid-State Difluoroboron Avobenzene. *J. Am. Chem. Soc.* **2010**, *132*, 2160–2162.
- (16) Galer, P.; Korosec, R. C.; Vidmar, M.; Sket, B. Crystal Structures and Emission Properties of the BF₂ Complex 1-Phenyl-3-(3,5-dimethoxyphenyl)-propane-1,3-dione: Multiple Chromisms, Aggregation- or Crystallization-Induced Emission, and the Self Assembly Effect. *J. Am. Chem. Soc.* **2014**, *136*, 7383–7394.
- (17) Louis, M.; Brosseau, A.; Guillot, R.; Ito, F.; Allain, C.; Métivier, R. Polymorphism, Mechanofluorochromism, and Photophysical Characterization of a Carbonyl Substituted Difluoroboron- β -Diketone Derivative. *J. Phys. Chem. C* **2017**, *121*, 15897–15907.
- (18) D'Aleo, A.; Felouat, A.; Heresanu, V.; Ranguis, A.; Chaudanson, D.; Karapetyan, A.; Giorgi, M.; Fages, F. Two-Photon Excited Fluorescence of BF₂ Complexes of Curcumin Analogues: Toward NIR-to-NIR Fluorescent Organic Nanoparticles. *J. Mater. Chem. C* **2014**, *2*, 5208–5215.
- (19) Li, X.; Liu, H.; Sun, X.; Bi, G.; Zhang, G. Highly Fluorescent Dye-Aggregate-Enhanced Energy-Transfer Nanoparticles for Neuronal Cell Imaging. *Adv. Opt. Mater.* **2013**, *1*, 549–553.
- (20) Pfister, A.; Zhang, G.; Zareno, J.; Horwitz, A. F.; Fraser, C. L. Boron Polylactide Nanoparticles Exhibiting Fluorescence and Phosphorescence in Aqueous Medium. *ACS Nano* **2008**, *2*, 1252–1258.
- (21) Contreras, J.; Xie, J.; Chen, Y. J.; Pei, H.; Zhang, G.; Fraser, C. L.; Hamm-Alvarez, S. F. Intracellular Uptake and Trafficking of Difluoroboron Dibenzoylmethane-Polylactide Nanoparticles in HeLa Cells. *ACS Nano* **2010**, *4*, 2735–2747.
- (22) DeRosa, C. A.; Seaman, S. A.; Mathew, A. S.; Gorick, C. M.; Fan, Z.; Demas, J. N.; Peirce, S. M.; Fraser, C. L. Oxygen Sensing Difluoroboron β -Diketone Poly(lactide) Materials with Tunable Dynamic Ranges for Wound Imaging. *ACS Sens* **2016**, *1*, 1366–1373.
- (23) Kerr, C.; DeRosa, C. A.; Daly, M. L.; Zhang, H.; Palmer, G. M.; Fraser, C. L. Luminescent Difluoroboron β -Diketone PLA-PEG Nanoparticle. *Biomacromolecules* **2017**, *18*, 551–561.
- (24) Kersey, F. R.; Zhang, G.; Palmer, G. M.; Dewhirst, M. W.; Fraser, C. L. Stereocomplexed Poly(lactic acid)-Poly(ethylene glycol) Nanoparticles with Dual-Emissive Boron Dyes for Tumor Accumulation. *ACS Nano* **2010**, *4*, 4989–4996.
- (25) Wilbraham, L.; Louis, M.; Alberga, D.; Brosseau, A.; Guillot, R.; Ito, F.; Labat, F.; Metivier, R.; Allain, C.; Ciofini, I. Revealing the Origins of Mechanically Induced Fluorescence Changes in Organic Molecular Crystals. *Adv. Mater.* **2018**, *30*, 1800817.
- (26) Yoskovitz, E.; Hadar, I.; Sitt, A.; Lieberman, I.; Banin, U. Interplay of Quenching and Enhancement Effects in Apertureless Near-Field Fluorescence Imaging of Single Nanoparticles. *J. Phys. Chem. C* **2011**, *115*, 15834–15844.
- (27) Krishna, G. R.; Kiran, M. S. R. N.; Fraser, C. L.; Ramamurty, U.; Reddy, C. M. The Relationship of Solid-State Plasticity to Mechanochromic Luminescence in Difluoroboron Avobenzene Polymorphs. *Adv. Funct. Mater.* **2013**, *23*, 1422–1430.
- (28) Seki, T.; Sakurada, K.; Ito, H. Controlling Mechano- and Seeding-Triggered Single-Crystal-to-Single-Crystal Phase Transition: Molecular Domino with a Disconnection of Auropilic Bonds. *Angew. Chem., Int. Ed.* **2013**, *52*, 12828–12832.
- (29) Genovese, D.; Aliprandi, A.; Prasetyanto, A.; Mauro, M. E.; Hirtz, M.; Fuchs, H.; Fujita, Y.; Uji-I, H.; Lebedkin, S.; Kappes, M.; De Cola, L. Mechano- and Photochromism from Bulk to Nanoscale: Data Storage on Individual Self-Assembled Ribbons. *Adv. Funct. Mater.* **2016**, *26*, 5271–5278.